Ceramics International **23** (1997) 497–507

PII: S0272-8842(96)00061-2
0272-8842/97 $17.00+.00

Experimental Characterisation of High Temperature Creep Resistance of Mullite

H. Rhanim,[a,b] C. Olagnon,[a] G. Fantozzi[a] & R. Torrecillas[c]

[a]Laboratoire GEMPPM, UMR CNRS 5510, bât. 502, INSA de Lyon, 20 bd. A. Einstein, 69621, Villeurbanne Cedex, France
[b]Faculté des sciences d'EL Jadida, département de physique, BP 20, EL Jadida, Morocco
[c]Instituto nacional del carbon, la corredoria, s/n. Apartado 73, 33080, Oviedo, Spain

(Received 13 November 1995; accepted 10 April 1996)

Abstract: The creep behaviour of mullite has been studied at temperatures between 1100°C and 1450°C. The two standard stages, primary and steady state are observed. The steady state strain creep rate may be represented by the standard relationship: $\dot{\varepsilon} = A\sigma^n \exp(-Q/RT)$ with a stress exponent value n equal to about unity and an activation energy Q of about 410 kJ/mol at low temperatures and up to 731 kJ/mol for temperatures above 1300°C. At high stress or temperature specimens failed. SEM observations of the fracture surface revealed that SCG played a major role in the failure process. The experimental lifetime values were compared to a simulation conducted by integration of $V-K_I$ laws determined by Double Torsion technique at 1200 and 1300°C. A fair agreement is observed suggesting that the creep duration is limited by SCG which causes the material failure, as assumed by Lange. © 1997 Elsevier Science Limited and Techna S.r.l.

1 INTRODUCTION

The increasing use of materials in high temperature structural applications requires a good knowledge of mechanical properties such as fracture strength, toughness and of even more importance the long term duration controlled by creep and subcritical crack growth.

Recently, dense polycrystalline mullite with little or nearly no glassy phase has become available by sintering fine mullite powders.[1] Although this material shows moderate flexural strength at high temperature, it remains a promising structural material owing to its high creep resistance in addition to its low thermal expansion.[2] However, the number of creep measurements on such material available in the literature is limited.[4,5,7,8,13]

The creep results are generally expressed in terms of deformation as a function of time. Although the mechanisms are different, most materials including metals and ceramics show the typical curve that is usually divided into three different parts called primary, secondary and tertiary creep. The secondary creep region is often designed as steady state creep since the creep rate is nearly constant. This region is therefore the most important for the understanding of the creep mechanisms.

The experimental data are generally characterized in terms of steady state creep rate according to the equation:

$$\dot{\varepsilon} = A\sigma^n \exp(-Q/RT) \quad (1)$$

where $\dot{\varepsilon}$ is the deformation rate, σ is the applied stress, n is the stress exponent, Q is the activation energy, T is the temperature and A is a material constant that depends on microstructure.

It has been shown that the values of n and Q depend on the creep mechanisms. For instance, deformation controlled by dislocations glide or climb, n can take on values ranging from $n = 3$ to $n = 8$. In the case of ceramics and for grain boundary sliding, n has been reported to be between 1 and 2 and creep controlled by diffusion is characterized by a stress exponent $n = 1$ and an activation energy equal to the activation energy for lattice diffusion (Nabarro–Herring creep) or to the activation energy for grain boundary diffusion (Coble creep).[17]

By fitting experimental results to eqn (1) it is possible to identify the deformation mechanisms.

In previous creep investigations on mullite, stress exponent values ranging from 1 to 1.4 were usually observed with an activation energy ranging from 700 to 1000 kJ/mol. These last values appear to be much larger than those observed for creep in other ceramic materials such as alumina, zirconia, and magnesia. Table 1 shows typical creep results of mullite found by different authors.

The objective of the present study was to evaluate the creep behaviour of mullite in order to gain insights into the mechanisms that control the deformation and failure of this material. For this purpose the influences of stress and temperature have been evaluated and related to microstructure evolution.

2 EXPERIMENTAL PROCEDURE

2.1 Material

The mullite used in this work was made by ITMA (Spain), from a Baikowski powder (CA 193 CR, France). Green compacts of mullite obtained by cold isostatic pressing under 200 MPa, were sintered for 2 h at 1750°C. A post treatment at 1450°C for 5 h was subsequently achieved in order to reduce the glassy phase content.

The density of the material measured by the Archimedes method is about 95.5%. The microstructure analysed by SEM on polished and thermal etched surfaces (Fig. 1) revealed two distributions of grain sizes: polyhedral grains with a size of 1–4 μm and elongated grains with long axis lengths of about 7 μm; one can also observe several pores at multiple-grain junctions. Transmission electron micrography (Fig. 2) revealed the presence of a glassy phase at the three-grain junction but since no high resolution was conducted, no intergranular glassy film has been observed.

Table 1. Some results on high-temperature creep of mullite

T (°C)	n	Q(kJ/mol)	Reference
1365–1480	1	870	[3]
1250–1290	1.1	360	[4]
1290–1360		1050	
1360–1430		750	
1400–1500	1	710	[5]
1350–1450	1	690	[6]
1400–1500	1.1 (1400) 1.4 (1500)	700	[7]

2.2 Creep experiment

The creep experiments have been conducted in bending, which offers two major advantages:

- A simple specimen geometry,
- A specimen jig that does not require the critical alignment needed in tension.

It also allows the possibility of testing many specimens and therefore under many different configurations for a relatively low cost. The drawbacks, however, is a stress field in the specimen which is not constant and therefore makes the analysis of the operating mechanisms rather difficult.

The use of compression whould have the same advantages. However, the creep rates are different[16] and the ultimate creep stage, where microcracking occurs, could not be observed.

The specimens, of shape 4×3×40 mm, were tested in four point bending with inner and outer spans equal to 18 and 36 mm, respectively. In all cases the tensile face of the specimens was polished down to 3 μm.

The constant load was applied through a dead load configuration, but a load cell (500N) present on the device allowed checking that the frictional forces remained negligible. The maximum deflexion was continuously recorded on the tensile face of the specimen using an alumina probe coupled with a displacement sensor. A detailed description of the measurement technique and creep apparatus is given elsewhere.[8]

The data analysis requires the knowledge of the stress and the strain. However, the stress field in the specimen is relatively complicated. Even under the hypothesis of a linear elastic material, the normal stress field in the specimen varies from compression to traction. When this hypothesis cannot

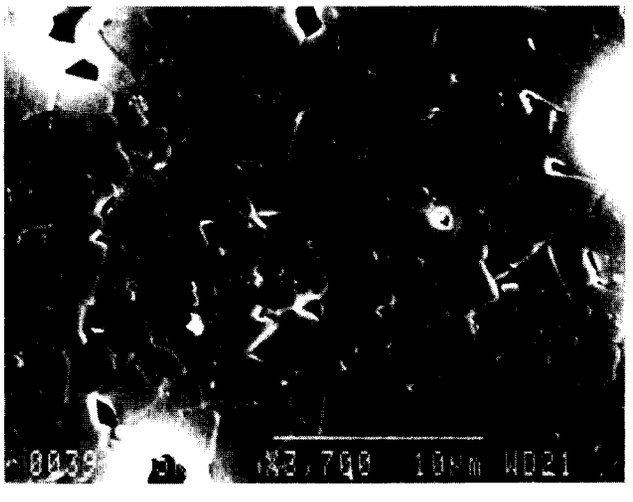

Fig. 1. Microstructure of thermal-etched surfaces of mullite (SEM).

be considered as relevant, i.e. when significant plastic deformation occurs, the evaluation of the stress and the deformation is even more complicated. Hollenberg[9] has proposed such an evaluation under the hypothesis that the neutral axis remained in the middle of the specimen. The results show that both the stress and the strain depend on the stress exponent n.

However, since the correction on the maximum tensile stress does not exceed 5%, we have calculated the stress according the linear elastic hypothesis:

$$\sigma = \frac{3P(L-l)}{2BW^2} \tag{2}$$

where P is the applied load, B the specimen breadth, W the specimen thickness and L and l the outer and inner span of the 4 point bending configuration, respectively.

The maximum strain in the specimen under the Hollenberg hypothesis is equal to:

$$\varepsilon = \frac{2W(n+2)}{(L-l)[L-l(n+1)]+1^2(n+2)/2} y_c \tag{3}$$

where y_c is the maximum deflexion.

3 RESULTS AND DISCUSSION

Figures 3–5 show some creep curves for mullite at several temperatures and stress conditions. After an elastic deformation recorded during the loading

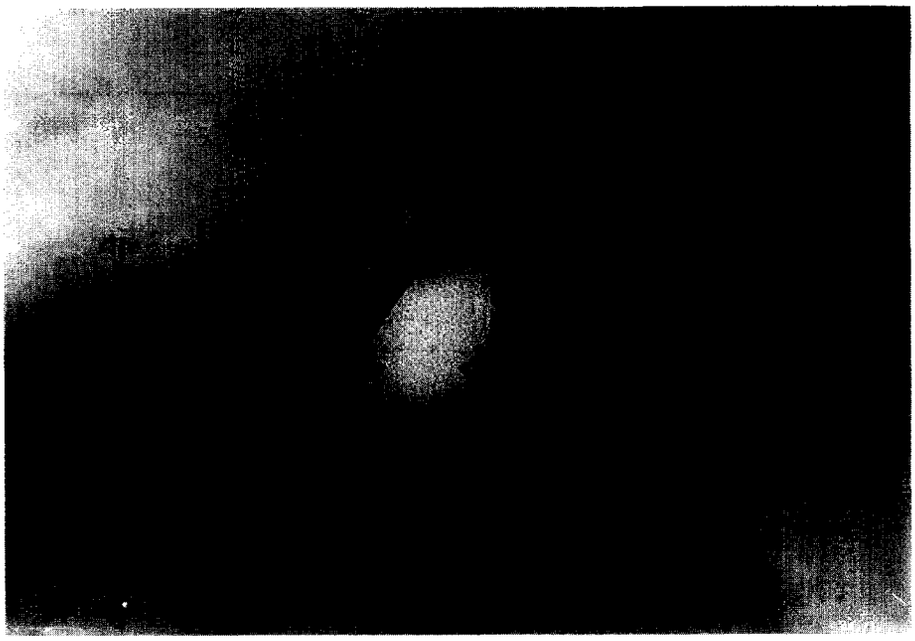

Fig. 2. Transmission electron micrograph showing glassy phase at triple points.

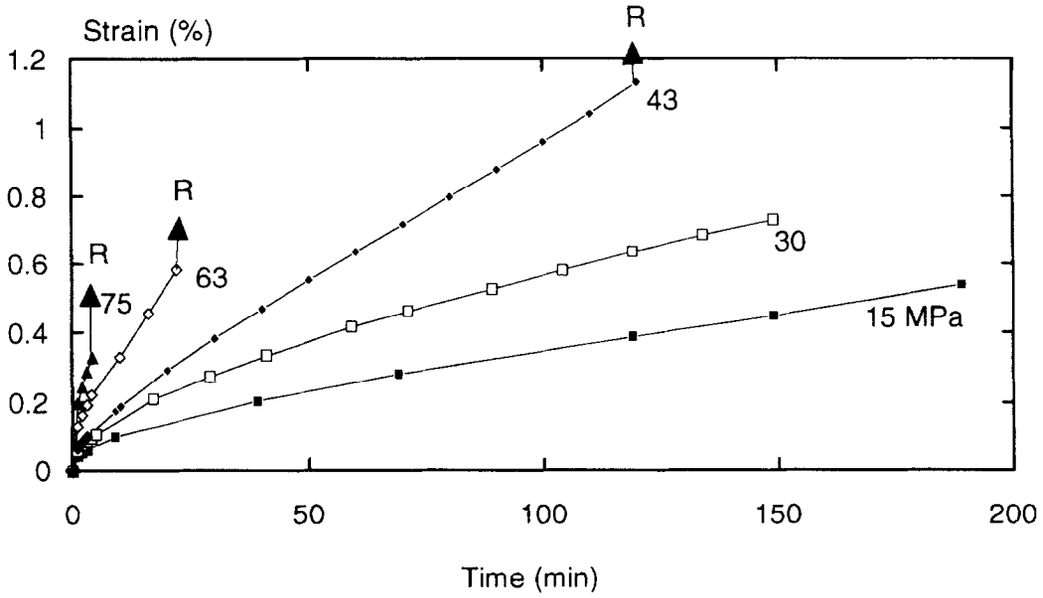

Fig. 3. Creep curves of mullite at 1450°C.

specimen period and a transient state where strain rate decreases with time, an apparently steady state is established. The evolution of strain rate with time during creep test in Fig. 6 shows that after a period of about 40 hours, the strain rate becomes approximately constant and one can then define a steady strain rate.

From these creep test results, one can note that:

- At 1100°C no specimen was broken after 85 h, deformations were relatively small and the steady strain rates were about 10^{-10} s^{-1}.
- At 1200°C, only specimens tested above 132 MPa were broken. For the other specimens the deformation after 85 h increases with increasing stress and the steady strain rate ranges from 4.5 10^{-10} to about 3 10^{-9} s^{-1}.
- At 1300°C specimens submitted to stresses above 75 MPa were broken and they exhibit a small deformation. One can also note that for specimens that did not fail, creep deformation after 85 h increases with increasing stress and strain rates were about 10^{-9} s^{-1}.
- At 1400°C, for stresses above 50 MPa specimens were broken with failure deformation decreasing with increasing stress and for stresses below 50 MPa the creep strain rate was about 10^{-8} s^{-1}.
- At 1450°C, specimens were broken under low stresses (40 MPa). The deformation for specimens tested below 40 MPa was relatively important. For example, under 15 MPa the deformation after 8.5 h, was 2.7% and the strain rate was about 10^{-7} s^{-1}.

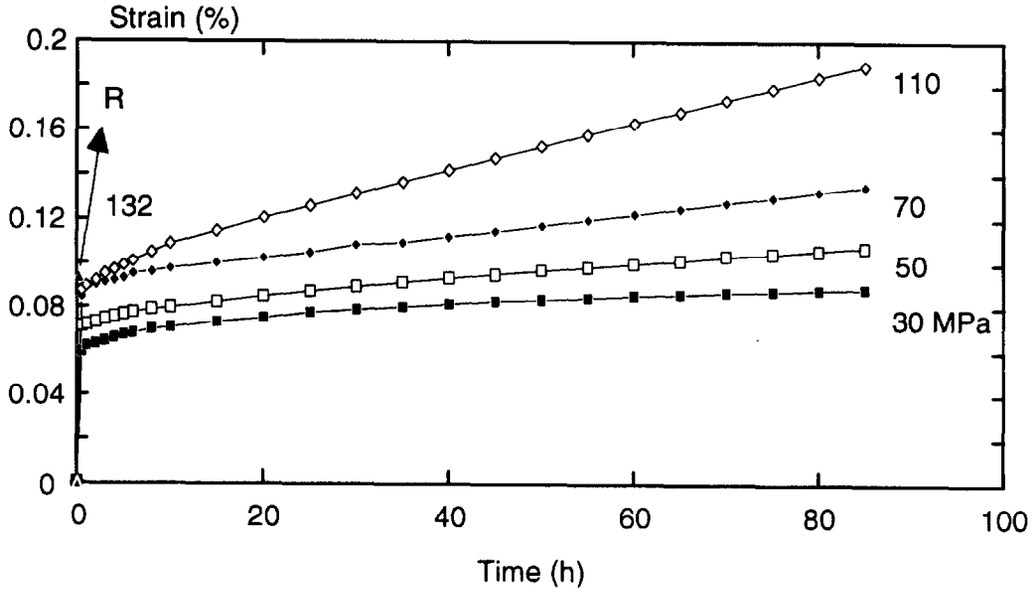

Fig. 4. Creep curves of mullite at 1200°C.

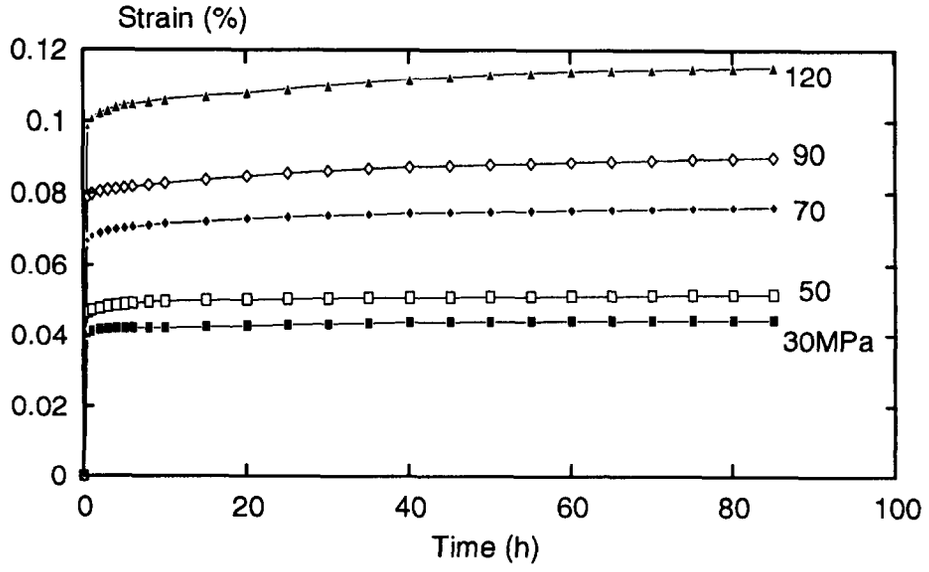

Fig. 5. Creep curves of mullite at 1100°C.

3.1 Stress effect

In order to determine the stress exponent which characterizes the stress effect on creep strain rate, the variation of steady strain rate with stress ($\log(\varepsilon) = f(\log\sigma)$) was plotted at different temperatures (Fig. 7). In the cases in which the specimens failed during the creep experiment the deformation rate at failure (i.e. minimum strain rate) has also been plotted.

One notes that for temperatures above 1100°C the curves can be defined by two apparent straight lines that correspond to two stress ranges which have been characterized by different stress exponents (Table 2).

One can note that the stress exponent n_2 in the second zone (where specimens failed during creep tests) decreases with increasing temperature. This may be explained by observing that as the temperature is raised the failure due to SCG occurred

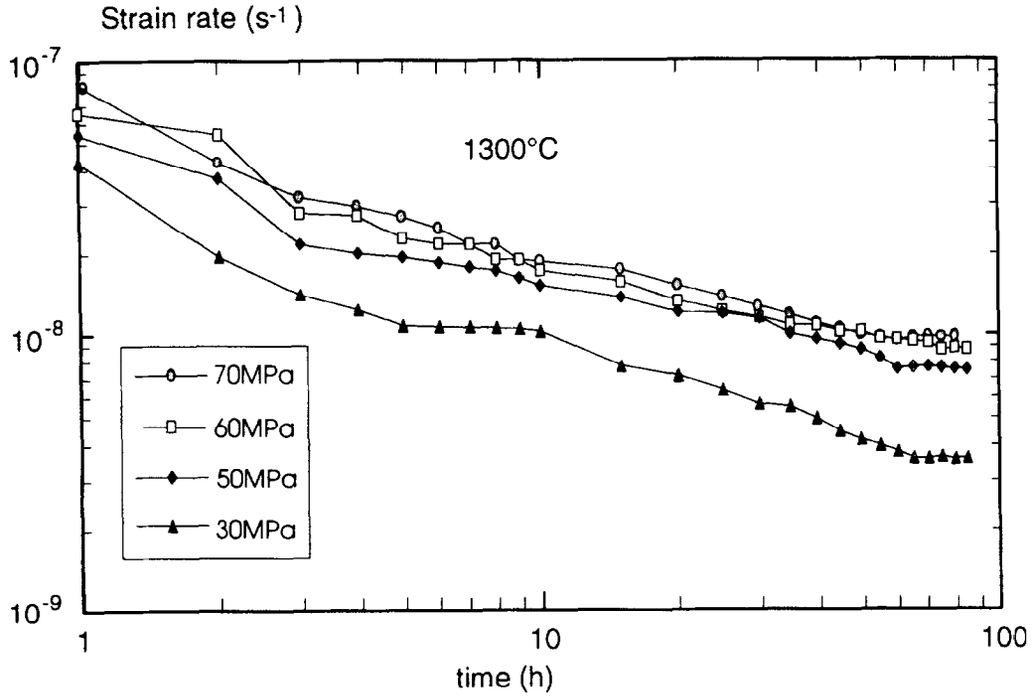

Fig. 6. Evolution of strain rate during creep test.

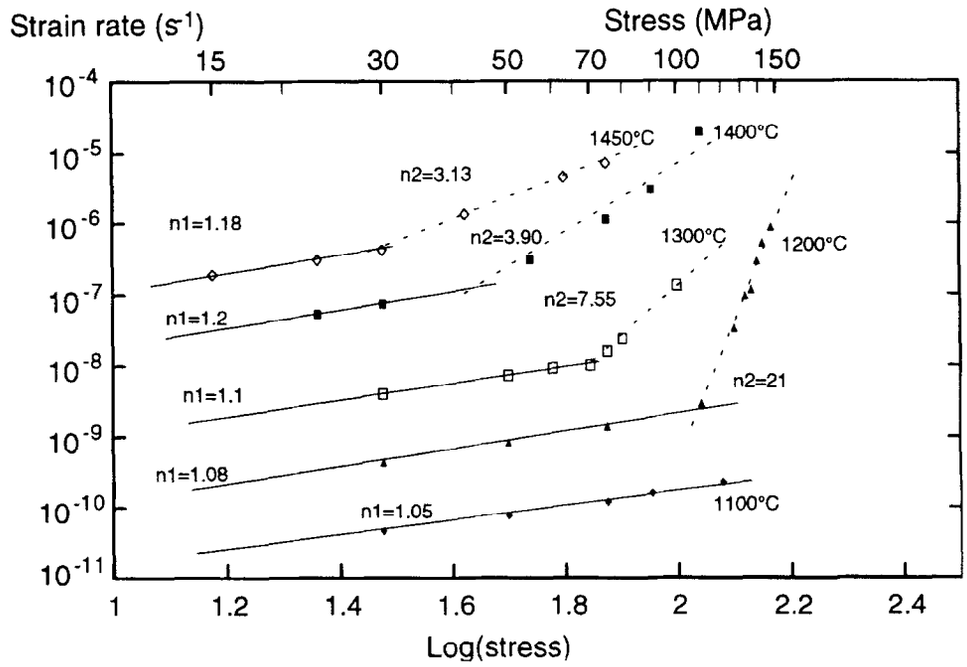

Fig. 7. Strain rate vs applied stress.

Table 2. Stress exponent values at different temperatures

Temperature (°C)	Stress exponent	
1100	n_1 =1.05	
1200	n_1 =1.08	for $\sigma \leq 110$ MPa
	n_2 =21	for $\sigma > 110$ MPa
1300	n_1 =1.1	for $\sigma \leq 70$ MPa
	n_2 =7.55	for $\sigma > 70$ MPa
1400	n_1 =1.2	for $\sigma \leq 50$ MPa
	n_2 =3.90	for $\sigma > 50$ MPa
1450	n_1 =1.18	for $\sigma \leq 30$ MPa
	n_2 =3.13	for $\sigma > 30$ MPa

at decreasing stresses. The failure therfore arises during later stages of transient creep closer to the steady state.

The value of n being nearly unity for creep of mullite at lower temperatures or at lower stresses and higher temperatures suggests a creep process controlled by a diffusional mechanism associated to viscous creep: either Coble (grain–boundary diffusion) or Nabarro–Herring (lattice diffusion), controlled by grain boundary sliding.

At high stresses a significantly higher value of the stress exponent n is observed. Care should be taken in the interpretation of these n values. The values of n at low stresses represent a stress dependence of the steady strain rate whereas the values of n at high stresses represent the stress dependence of the strain rate at which specimen fracture occurred. It may then be questionned whether these high values of n are a true stress effect or whether it is brought about by overvaluation of the steady creep rate. The answer is suggested by Fig. 8 where one can clearly note that the specimens failed during the transient state.

It can also be noted that the value of a transition stress between those two parts decreases with increasing temperature.

3.2 Temperature effect

The temperature dependence of the strain rate is shown in Fig. 9 for three applied stresses. This plot indicates that for lower temperatures activation energy for creep deformation was about 410 kJ/mol independently of the applied stress, while it increased with increasing stress for higher temperatures. It varied from 731 kJ/mol at 30 MPa to 930 kJ/mol at 70 MPa. It is important to note however that for 50 and 70 MPa, the specimens failed during the primary stage. Nevertheless those values of activation energy appear to be of the order of values reported by other authors (Table 1).

3.3 Analysis and discussion

In order to determine the mechanisms governing creep deformation SEM observations were conducted to investigate the microstructure and damage after creep tests on both failure and tensile surfaces. No apparent change in microstructure from was observed for the tensile surface of the specimen after the creep test. Nevertheless we have observed an increase in the number of triple junction voids for specimens crept at higher temperatures (Fig. 10). On the other hand we have

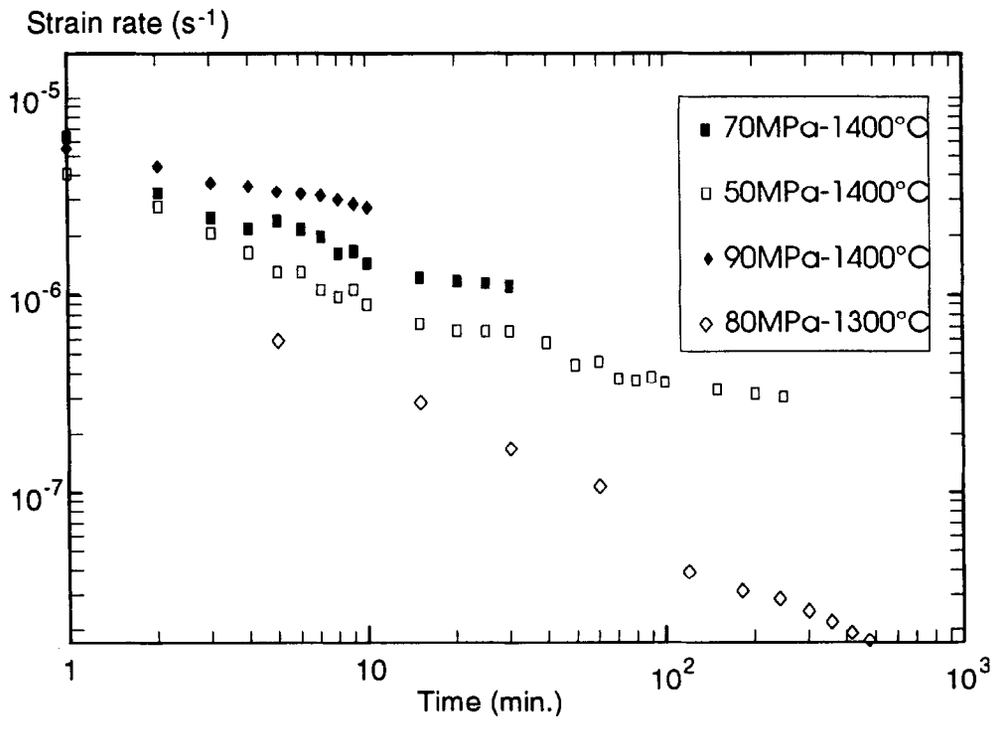

Fig. 8. Evolution of strain rate during creep test showing failure in the transient stage.

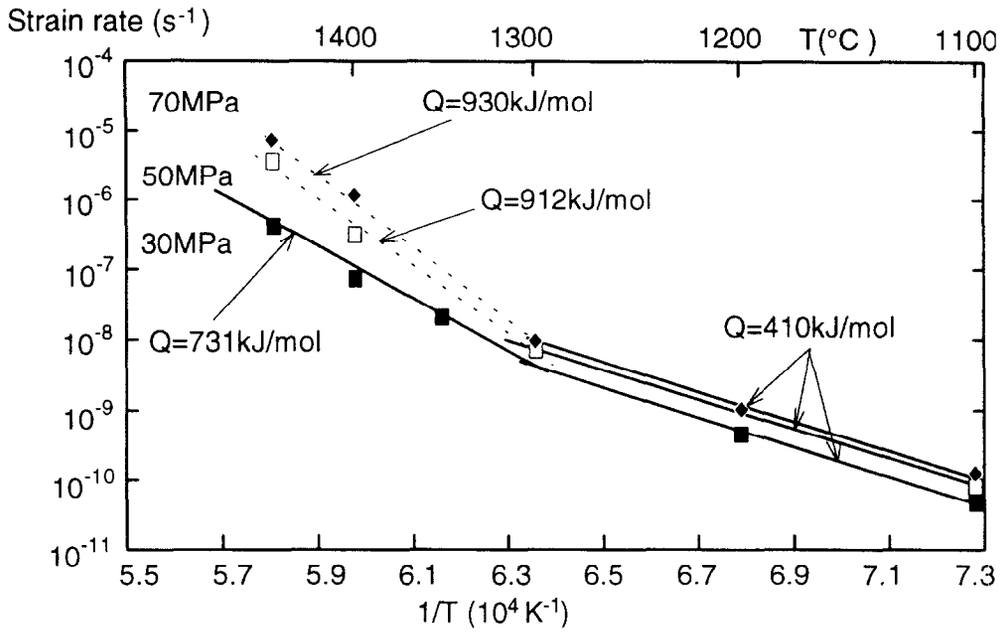

Fig. 9. Temperature dependance of creep strain rate.

observed an intrusion/extrusion of grains on the surfaces of crept specimens. This phenomenon had also been observed by Gros[8] and Dokko[5] who considered it as an indication of the occurrence of grain boundary sliding.

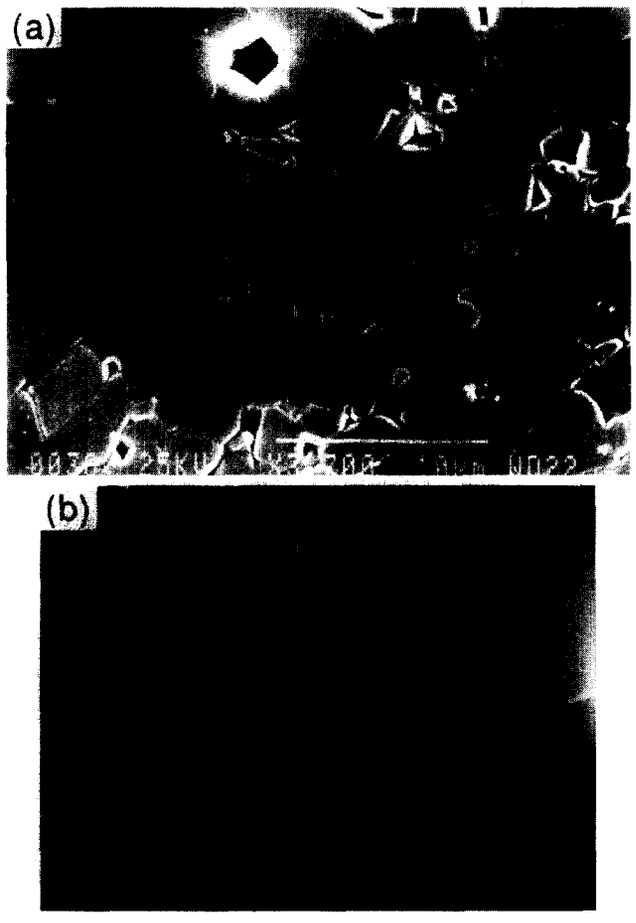

Fig. 10. Tensile surface after creep test at 1450°C and 30 MPa (indicating some change in microstructure).

The values of stress exponent, ranging from 1.05 to 1.2 in the first part, are in good agreement with those found by different authors (Table 1). It was generally suggested that the creep deformation was controlled by a diffusional mechanism. In addition Dokko[5] found that the grain size exponent defined by $\dot{\varepsilon} = \frac{\sigma^n}{d^p}$ was about two suggesting a Nabarro–Herring diffusion mechanism. However, for the mullite investigated in this work, the authors believe that the deformation is controlled by a viscous creep or grain boundary sliding.

The theoretical models of creep diffusion suggest an increase of grain size during creep test and in order for the grains to maintain compatibility during the deformation an accommodation process must occur. Raj[10] has proposed that diffusion and grain boundary sliding are coupled mechanisms which are accommodated mutually.

In the present material accommodation by grain boundary sliding is considerably limited because of the larger grains and the small amount of intergranular phase. It may therefore be assumed that a swinging movement of grains is responsible for triple junction cavity formation and intergranular separations of larger grains, as discussed by Moussa.[11] Fig. 11.

We have also observed some facet-sized cavities created by growth and coalescence of several cavities at two grain junctions on the tensile surface of specimens crept to 2.7% under 15 MPa and 1450°C (Fig. 11).

The small increase of n-value from 1.05 to 1.2 with increasing temperature suggests that the relative contribution of non-Newtonian creep to the total creep rate increases with temperature. This is

in agreement with the fact that at lower temperatures no change in microstructure after creep tests was noted.

Concerning the temperature effect on creep strain rate, at lower temperatures one can say that the creep occurs by small grain movement (GBS or Swinging), entirely accommodated by a viscous creep through the amorphous grain boundary phase. The absence of modification in microstructure and the stress exponent equal to 1.05 confirms this hypothesis.

For specimens tested under low stress, the increase in activation energy at high temperatures is an indication of a change in deformation mechanism probably caused by the decrease of the intergranular phase viscosity, making the grain movement easier. It also induces cavity formation at triple junctions and at mullite–mullite grain boundaries. The strong increase in activation energy at high temperatures with increasing stress might be explained by the high creep rate values of specimens which failed in the transient stage.

As already said the specimens belonging to the second part of the $\dot{\varepsilon}$–σ graphs (Fig. 7) exhibit a small failure deformation. SEM observations of the fracture surfaces clearly revealed two zones. Intergranular fracture is predominant near the tensile surface while transgranular fracture is predominant in the second zone (Fig. 12). This reveals the existence of SCG followed by fast fracture, which suggests that the crack growth process plays an important role and controls the fracture. As stress decreases, the size of this intergranular zone increases. For example, the fracture surface of a specimen crept at 50 MPa and 1450°C shows intergranular fracture on the whole surface. Using the applied stress and the size of these intergranular zones, the fracture toughness was calculated approximately. The values are given in Table 3. These values are in fair agreement with those generally measured in mullite by the standard SENB method, i.e. about twice those obtained at room temperature.[13]

These different observations lead us to think that failure is the result of two independent mechanisms: the accumulation of creep damage and slow crack growth. Such SCG and creep fracture were governed by grain boundary separation and sliding mechanisms. Lange[12] has proposed a simple analysis to describe the concomitant processes of creep and SCG that has been shown to operate in several

Fig. 11. Facet-sized cavity created by growth and coalescence of several cavities (specimen crept to 2.7% under 15 MPa and 1450°C).

Table 3. Size of intergranular zones at different test conditions and related stress intensity factors

Test conditions	Size of intergranular zone (mm)	K_{IC} (MPa m$^{1/2}$)
1200°C and 132 MPa	0.364	3.6
1300°C and 100 MPa	1.654	4.1
1400°C and 110 MPa	1.13	3.8
1400°C and 90 MPa	1.9	3.9
1450°C and 75 MPa	0.838	3.8

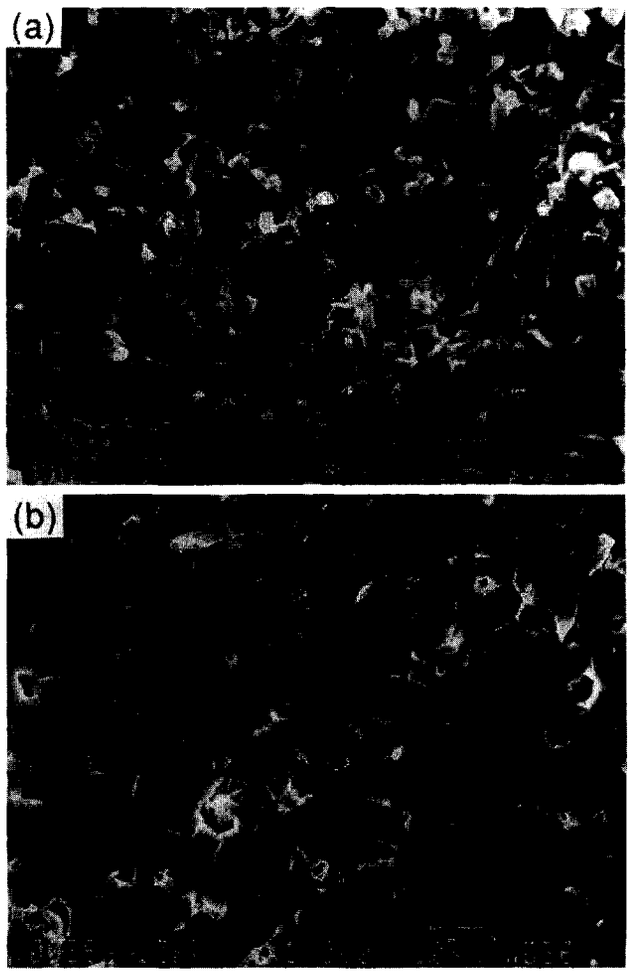

Fig. 12. SEM of surface fracture after creep at 1400°C, 110 MPa. (a) Intergranular fracture zone; (b) transgranular fracture zone.

materials.[14] It is based on the hypothesis that the creep duration is limited by the time taken for a crack to grow up to the critical size which leads to failure. The analysis is therefore the following:

- Creep is governed by the standard equation:

$$\varepsilon = \varepsilon_0 + A\sigma^n t \tag{4}$$

where only the steady state creep is considered.

- SCG is also described by the standard equation:

$$V = BK^m \tag{5}$$

where B and m are constant.

The time to failure due to SCG under static loading is given by[15]:

$$t_f = \frac{2c_i^{(2-m)/2}}{(m-2)BY^m}\sigma^{-m} \tag{6}$$

where c_i is the initial crack length and Y is the stress intensity geometrical factor.

By reporting t_f in the creep deformation equation (4) one obtains the creep strain at failure:

$$\varepsilon_f = \varepsilon_0 + \frac{2c_i^{(2-m)/2}A}{(m-2)BY^m}\sigma^{n-m} \tag{7}$$

One can also obtain a relationship between the time to failure and the creep rate:

$$t_f = A^{m/n}\frac{2c_i^{(2-m)/2}}{(m-2)BY^m}\dot{\varepsilon}^{-m/n} \tag{8}$$

From the plot of (7) and (8), one can obtain a general estimation of the exponent values, n and m, of the two basic mechanisms. Unfortunately, although the basic hypothesis is relevant, one cannot use these equations because in this case the failure occurred mostly in the primary stage where eqn (1) is not valid.

The same approach with a different methodology has therefore been used to demonstrate that the fundamental Lange hypothesis gives a correct description of the mechanical behavior. The idea was first to record the SCG behaviour by double torsion technique. This has been achieved at 1200°C and 1300°C (Fig. 13) on the same material (experimental details are published elsewhere).[18] The lifetime under static loading at 1200 and 1300°C was subsequently evaluated by integration of the DT law. It should be pointed out that the different crack velocity stages present in Fig. 14 have been considered. These simulation results are represented in Fig. 14 and compared to the experimental values obtained during creep experiments.

For the higher stress regime, a good agreement is observed suggesting that the creep curves are indeed limited by the SCG which could imply that the two mechanisms operate in parallel.

4 CONCLUSION

A systematic experimental characterisation of creep resistance of mullite was performed at temperatures between 1100°C and 1450°C under several stresses. This study indicates clearly that this

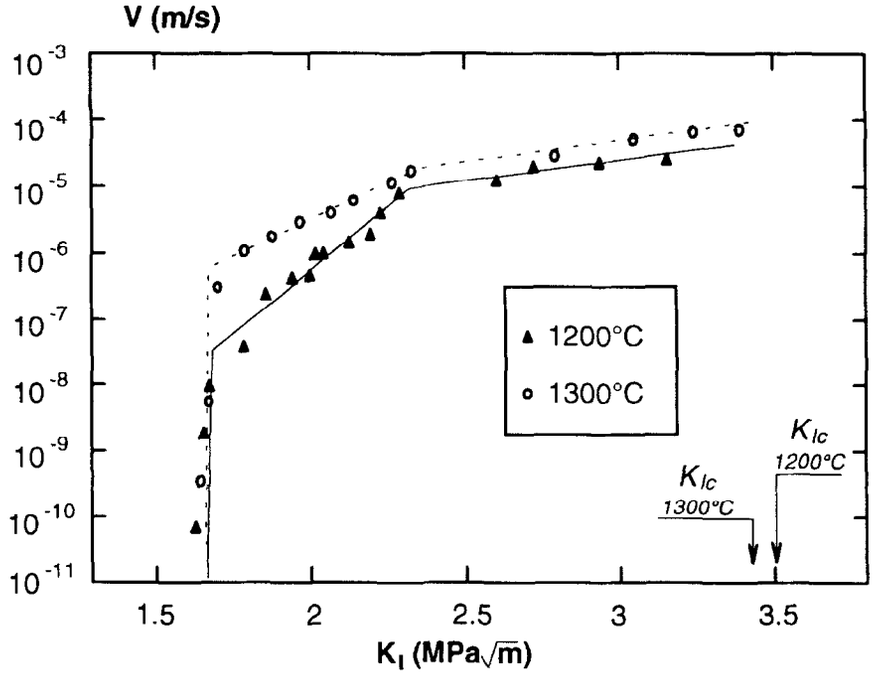

Fig. 13. V–K_I diagram for mullite (obtained by DT technique).

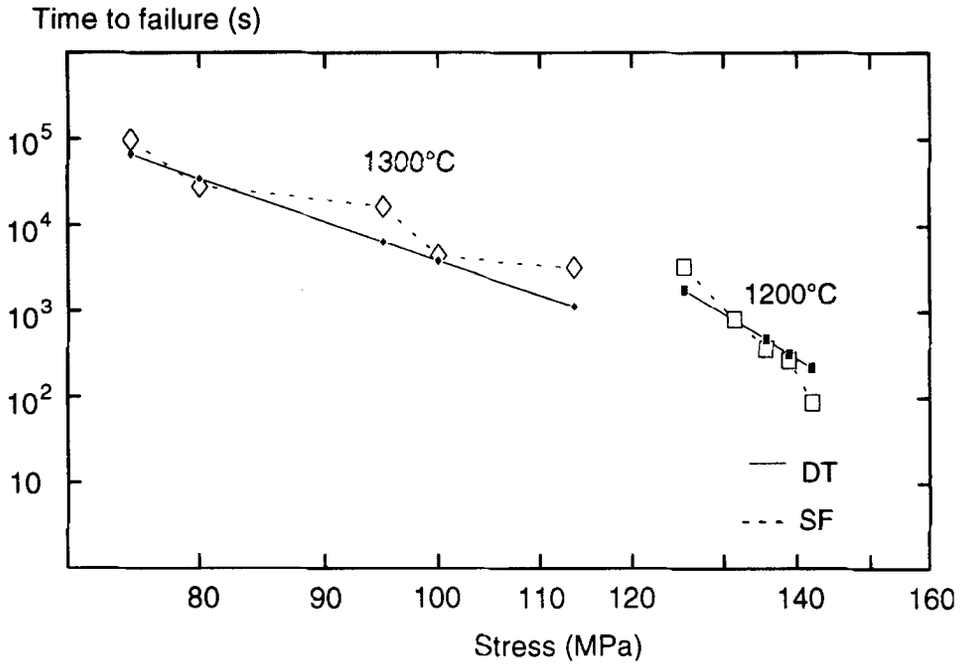

Fig. 14. Time to failure obtained by both methods (double torsion and static fatigue).

material exhibits, concurrently, creep and slow crack growth.

- An effective transition stress exists at each temperature. Above this stress the specimens failed in transient state and then the apparent stress exponent was enhanced to a value n_2 which decreases strongly with temperature increase.
- Below the transition stress, the creep rate was characterized by a stress exponent close to unity, suggesting a viscous creep. For lower stresses, the activation energy was about 410 kJ/mol at low temperatures and it increases until 731 kJ/mol for higher temperatures.
- For specimens failed during creep tests, the lifetime under static loading was evaluated by integration of SCG laws which were determined by DT technique at 1200 and 1300°C.These simulation results seem in a fair agreement with the experimental values suggesting that the Lange hypothesis is verified and the creep duration is limited by SCG, which causes the material failure.

REFERENCES

1. OHNISHI, H., *et al.*, Mechanical properties of mullite. *2nd Int. Symp. on Ceramic Materials and Component for Engines*, Lübeck, Germany, 1986, pp. 633–641.
2. MIZUNO, M., Microstructure, microchemistry, and flexural strength of mullite ceramics. *J. Am. Ceram. Soc.*, **74**(12) (1991) 3017–3022.
3. OKAMOTO, Y., Creep deformation of polycrystalline mullite. *J. Eur. Ceram. Soc.*, **6** (1990) 161–168.
4. KOESTER, D. A., *et al.*, High temperature creep of SiC whisker reinforced ceramics. *Whisker and fiber toughened ceramics, Proc. Int. Conf.*, Oak Ridge Tennessee, USA June 1988, pp. 139-145.
5. DOKKO, P. C., High temperature mechanical properties of mullite under compression. *J. Am. Ceram. Soc.*, **60**(3/4) (1977) 150–155.
6. LESSING, P. A., Creep of polycrystalline mullite. *J. Am. Ceram. Soc.*, **58**(3/4) (1975) 149–150.
7. PENTY, R. A. & HASSELMAN, D. P. H., Creep kinetics of high purity, ultrafine grain polycrystalline mullite. *Mater. Res. Bull.*, **7** (1972) 1117–1124.
8. GROS, H., Etude du comportement en fluage haute temperature de ceramiques à base alumine, mullite et zircon. PhD Thesis, INSA de Lyon, France, 1991.
9. HOLLENBERG, G. W., TERWILLIGER, G. R. & GORDON, R. S., Calculation of stresses and strains in four-point bending creep tests. *J. Am. Ceram. Soc.*, **54**(4) (1971) 196–199.
10. RAJ, R. & ASHBY, M. F., On grain boundary sliding and diffusionnal creep. *Metall. Trans.*, **2**(4) (1971) 1113–1127.
11. MOUSSA, R., Contribution à l'étude du comportement en fluage de materiaux SiC. PhD Thesis, Université de Caen, France, 1985.
12. LANGE, F. F., Interrelations between creep and slow crack growth for tensile loading conditions. *Int. J. Fracture*, **12**(5) (1976) 739–744.
13. TORRECILLAS, R., Comportamiento mecanico de mullita y mullita-circona obtenida por sinterizacion reactiva. These de Doctorat: UNED, Madrid, 1990.
14. SAMADDAR, S.S., OLAGNON, C. & FANTOZZI, G., Interaction between creep and slow crack growth in the process of high temperature failure of mullite zirconia at 1400°C, to be published.
15. RITTER, J. E., Jr, Engineering design and fatigue failure of brittle materials. In *Fracture Mechanics of Ceramics, Vol. 4, Crack Growth and Microstructure*, ed. R. C. Bradt, D. P. H. Hasselman & F. F. Lange. New York, 1978, pp. 667–686.
16. MORRELL, R. & ASHBEE, K. H. G., High temperature creep of lithium zinc silicate glass-Ceramics 1. General behavior and creep mechanisms. *J. Mater. Sci.*, **8** (1973) 1253–1270.

17. RUANO, O. A. & SHERBY, O. D., On constitutive equation for various diffusion-controlled creep mechanisms. *Revue Phys. Appl.*, **23** (1988) 625–637.
18. RHANIM, H., OLAGNON, C., FANTOZZI, G. & TORRECILLAS, R. Crack propagation behaviour of mullite at high temperatures by Double-Torsion technique, *J. Eur. Ceram. Soc.*, **17** (1997) 85–89.